

Review

Metal Additive Manufacturing for Satellites and Rockets

Tomasz Blachowicz ¹, Guido Ehrmann ² and Andrea Ehrmann ^{3,*}

¹ Institute of Physics—Center for Science and Education, Silesian University of Technology, 44-100 Gliwice, Poland; tomasz.blachowicz@polsl.pl

² Virtual Institute of Applied Research on Advanced Materials (VIARAM); guido.ehrmann@gmx.de

³ Faculty of Engineering and Mathematics, Bielefeld University of Applied Sciences, Interaktion 1, 33619 Bielefeld, Germany

* Correspondence: andrea.ehrmann@fh-bielefeld.de

Abstract: The emerging technology of 3D printing can not only be used for rapid prototyping, but will also play an important role in space exploration. Additive manufactured parts can be used in diverse space applications, such as magnetic shields, heat pipes, thrusters, etc. Three-dimensional printed parts offer reduced mass, high possible complexity, and fast printability of custom-made objects. On the other hand, materials which are not excessively damaged by the harsh conditions in space and are also printable by available technologies are not abundantly available. This review gives an overview of recent metal additive manufacturing technologies and their possible applications in space, with a focus on satellites and rockets, highlighting already applied technologies and materials and gives an outlook on possible future applications and challenges.

Keywords: powder bed fusion; microsattellites; thrusters; structural components; space flight; aerospace; aeronautics



Citation: Blachowicz, T.; Ehrmann, G.; Ehrmann, A. Metal Additive Manufacturing for Satellites and Rockets. *Appl. Sci.* **2021**, *11*, 12036. <https://doi.org/10.3390/app112412036>

Academic Editors: Ricardo Branco, Filippo Berto and Rui C. Martins

Received: 10 November 2021

Accepted: 14 December 2021

Published: 17 December 2021

Publisher's Note: MDPI stays neutral with regard to jurisdictional claims in published maps and institutional affiliations.



Copyright: © 2021 by the authors. Licensee MDPI, Basel, Switzerland. This article is an open access article distributed under the terms and conditions of the Creative Commons Attribution (CC BY) license (<https://creativecommons.org/licenses/by/4.0/>).

1. Introduction

Additive manufacturing (AM), also called 3D printing, belongs to the emerging technologies of our time. After being used for rapid prototyping at the beginning, current rapid production is enabled for many applications due to increasingly improved technologies.

While the technologies of fused deposition modeling (FDM) or stereolithography (SLA) are most often used in the low-cost sector to print 3D shapes from diverse polymers [1], technologies such as selective laser melting (SLM), selective laser sintering (SLS), electron beam melting (EBM), and direct energy deposition (DED) can even be used to form metal products [2].

Besides fast production without the necessity to prepare a time- and cost-intensive injection mold beforehand, additive manufacturing has the advantages of allowing preparation of nearly unlimited shapes, including diverse forms which could not be produced by common techniques such as injection molding, and thus of building lighter and nevertheless stable objects [3,4]. On the other hand, the mechanical properties of the 3D printed objects may be reduced in comparison with other manufacturing methods due to layerwise production, and residual stress and deformation may cause problems in the application of additively manufactured parts [5,6].

While these aforementioned problems must be overcome by careful process engineering, additive manufacturing is especially interesting for aerospace applications where fast development and mass reduction are of high importance [7]. Another reason why additive manufacturing is important for space applications, e.g., of satellite and rocket parts, is the possibility to prepare custom-made objects at a high speed of production, without the necessity to prepare expensive molds beforehand. This article thus gives, after a brief introduction of the most common metal additive manufacturing methods, an overview of possible applications of metal AM for modern aeronautics, as they are investigated in recent

research studies and already applied. Finally, it summarizes the remaining challenges and indicates possible future applications.

The paper is organized as follows. Starting with an overview of diverse metal additive manufacturing techniques, applications for microsattellites, such as thrusters, structural components, and antennas, are described together with a few other applications reported in the literature. Each section contains applications at the laboratory stage, where basic research is necessary to evaluate the potential for future applications, along with mature applications which are already used in actual satellites and rockets. Finally, future potential applications are described.

2. Metal Additive Manufacturing Techniques

While polymer 3D printing usually works by placing a molten filament on the desired positions or polymerizing a liquid resin at defined places, metal additive manufacturing is usually based on metal powders or even metal wires. Typical materials used for metal AM include aluminum, stainless steel, titanium, or cobalt chrome [8]. According to ASTM standard F2792 [9], metal AM processes can be subdivided into powder bed fusion and directed energy deposition.

Powder bed fusion processes generally include a powder bed in which energy is deposited at defined positions to either melt or sinter the metal powder by a laser or an electron beam. As an example, Figure 1 depicts the process of selective electron beam melting (SEBM) [10]. The four-step process starts with the application of a powder layer, which is heated, molten, until the layer is fully produced, and the platform can be lowered to enable application of the next powder layer.

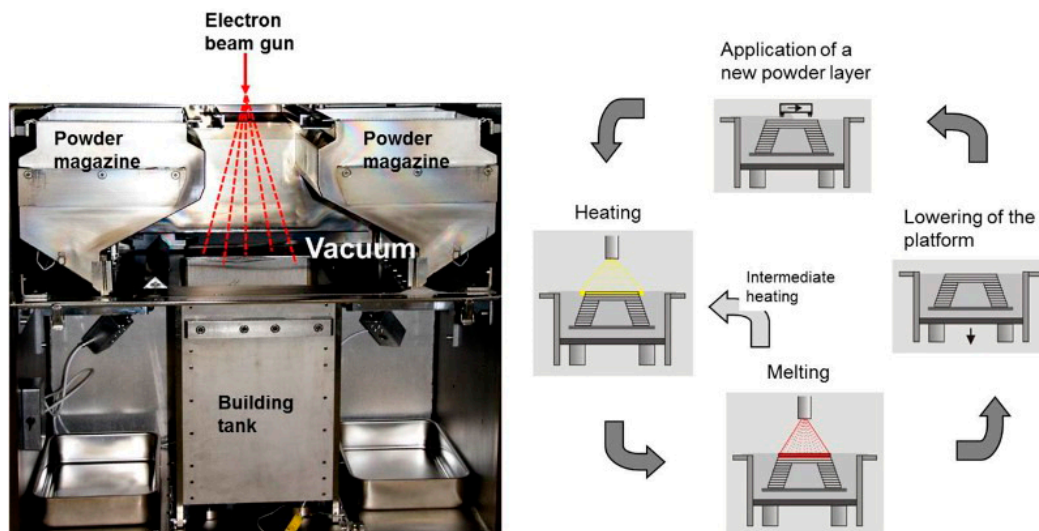


Figure 1. Selective electron beam melting process. **Left:** Process chamber. **Right:** 4-step process for building one layer. From [10], originally published under a CC-BY license.

It must be mentioned that the process works in “controlled vacuum”, i.e., the chamber is pumped to approximately 10^{-4} to 10^{-5} mbar before helium is inserted to reach a low pressure of about 10^{-3} mbar, to prevent electrostatic charging [10]. Electrons are emitted from a tungsten filament or a LaB_6 cathode and, as in scanning electron microscopy, are accelerated and focused using electromagnetic lenses [11]. The object is built in layers of typical thicknesses between 0.05 and 0.15 mm. Generally, a new powder layer is preheated to temperatures between 300 and 1100 °C for different metals to start sintering, e.g., to around 400 °C for pure copper and 900–1100 °C for Ti–48Al–2Cr–2Nb powder [12,13], in this way increasing the electrical conductivity and thus avoiding repulsion of charged powder particles [14], then melted where desired, lowering the platform, applying a new powder layer of defined thickness on the platform, and starting with the next preheating

step. Literature reports indicate that selective electron beam melting results in relatively coarse surfaces and internal microstructures [15], but on the other hand in low residual stress [16].

Besides selective electron beam melting, there are several laser-based processes that work with a powder bed. One is the aforementioned selective laser melting (SLM), using a laser to fully melt the powder, in this way creating dense layers so that no post-treatment (as in SLS) is necessary [17]. Instead of the electron beam described previously, here a laser beam scans the surface, focused with normal glass lenses. SLM usually works in a nitrogen or argon atmosphere to avoid oxidation during the fusion process, with nitrogen having a larger thermal conductivity, which is advantageous for cooling the specimens that are produced [18,19]. The SLS process is in principle identical, with a different nature of powder fusion [20]. The process and the melt pool formation are depicted in Figure 2 [20]. Similar to the aforementioned selective electron beam melting, here a laser beam is used to melt the powder in the upper layer, before the build plate is lowered, and a new powder layer is placed in the build area by the recoater (Figure 2a). The geometry of the melt pool, produced by laser heating, is depicted in detail in Figure 2b.

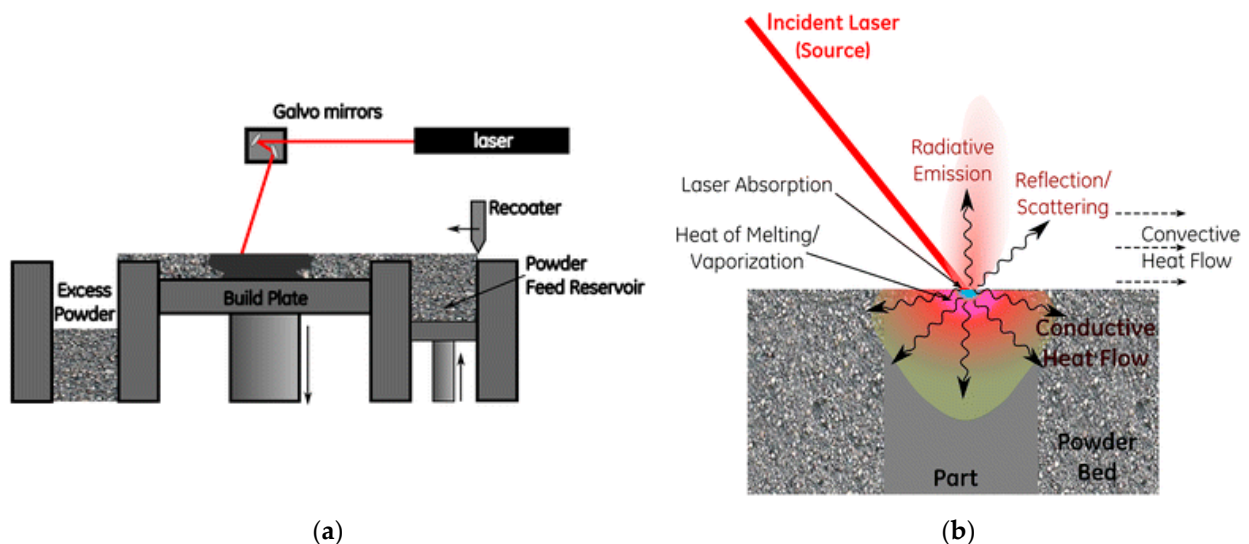


Figure 2. (a) Typical SLM or SLS process; (b) heat transfer paths in melt pool formation and solidification in an SLM process. From [20], originally published under a CC-BY license.

In addition to these typical powder bed fusion processes, there are also directed energy deposition (DED) processes used for metal additive manufacturing. Figure 3 depicts two typical DED systems [21], working with a laser or electron beam and powder or wire feed, respectively. In both cases, the material used to build an object is deposited only at the required position, either as a powder (Figure 3A) or as a wire (Figure 3B), opposite to the aforementioned powder bed processes where the powder is provided along the whole building area. These materials are again heated by laser (Figure 3A) or electron beam (Figure 3B), similar to the aforementioned techniques.

Electron-DED again works in vacuum, while laser-based DED systems use inert gases as described for the powder bed fusion processes. In the powder-based DED systems, an inert gas can be introduced into the melting region together with the metal powder (Figure 3A). It is even possible to use multiple nozzles for powder introduction so that objects can be prepared from material mixtures, differing along the specimen [22]. It is also possible to use plasma as the energy source, such as gas metal arc welding [23]. Generally, laser- and plasma-produced parts usually need post-treatment due to high residual stress in the specimens, which has to be relieved and the necessity to improve the microstructure, while stress is usually lower for electron-beam produced parts which are nearly fully densely produced [24].

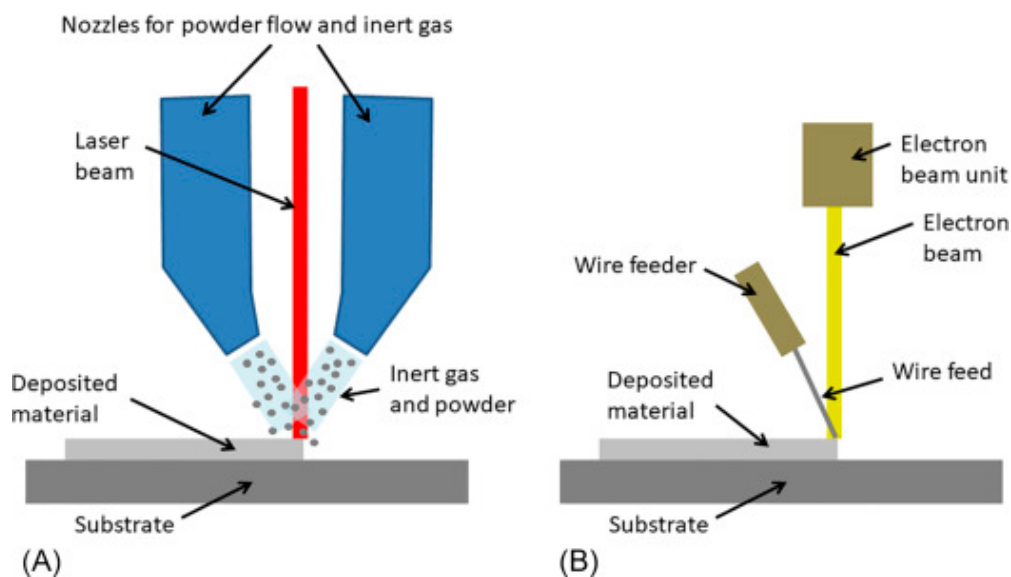


Figure 3. Schematics of two directed energy deposition (DED) systems: (A) DED system using laser with powder feedstock; (B) DED system using electron beam and wire feedstock. Reprinted from [21], with permission from Elsevier.

Another additive manufacturing technique working with a wire is the wire-arc additive manufacturing (WAAM), in which a wire feed is molten by an electric arc source, allowing for additive manufacturing of steel and several alloys [25,26].

Additionally, it should be mentioned that some of the alloys which are highly interesting for space applications have been processed with especially well-suited metal additive manufacturing methods. A compositionally graded alloy from CoCrMo and Inconel 718, enabling fitting the material at each position to the required working conditions, was produced by laser powder bed fusion [27]. SEBM is often used to prepare Ni-based superalloys for high-temperature applications [28].

Generally, it must be mentioned that the morphological properties of additively manufactured specimens can significantly differ from the designed structures, and the mechanical properties can show large deviations from the wrought material due to the inclusion of air voids or other microstructural differences [29,30]. Other problems related to the different methods are the aforementioned necessity to work in vacuum or inert gas atmosphere and the often highly challenging parameter optimization for each new material, including different batches of nominally identical materials. Furthermore, each material has different challenges, such as the problem of hot cracking at grain boundaries in Ni-based superalloys, occurring during the final solidification stages [31].

As this brief overview of some common metal additive manufacturing methods shows, there are diverse techniques available with different advantages and challenges, which are steadily being developed for using metal additive manufacturing in increasingly more applications. The next sections give an overview of possible applications in aerospace research and industry.

3. Microsatellites

Microsatellites have emerged during the last few years since they are relatively inexpensive and can be used for a broad range of applications [32,33]. There have been diverse attempts to use 3D printing techniques for different parts of microsatellites, using polymers, metals, and hybrid materials, which were previously reviewed by our group [34], so that here only a brief overview of the most recent reports is given.

Funase et al. reported on a water resistojet thruster system called “Aquarius” for the EQUULEUS CubeSat, which is planned to explore the Earth–Moon Lagrange point, whose vaporization chamber is prepared from the aluminum alloy AlSi₁₀Mg and in which the cavity and flow paths are produced by additive manufacturing by a not-nearer defined

technique [35]. The same material was used for selective laser melting of a whole CubeSat structure to improve the accessibility to internal components by using a modular backplane system [36].

Yendler et al. prepared a thermal management system for high power CubeSats to reach effective heat dissipation and used additive manufacturing by ultrasonic welding combined with CNC subtractive manufacturing for the preparation of the whole system, consisting of a rollout deployable radiator, a phase change material based thermal accumulator, and structurally integrated heat pipes [37].

In his dissertation thesis, working on a CubeSat power management subsystem for the ALSat#1 mission, Panagopoulos reports that one of the partners of the consortium uses metal additive manufacturing for the structural design of the satellite, without more specific information about the exact technique [38]. A CubeSat structure was also reported to be manufactured using selective laser sintering [39].

An antenna for low-Earth orbit microsattellites, produced by electron beam melting, was reported by Arnaud et al. [40]. Similarly, metasurface antennas especially for CubeSats and SmallSats were built by metal additive manufacturing combined with CNC milling [41]. Larger structures, such as a solar panel, were prepared by SLM, allowing for printing a double-layer aluminum structure with I-shaped beams (Figure 4), which was found to show significantly increased shielding, improved mechanical properties, and reduced mass, as compared to a conventional aluminum honeycomb panel [42].

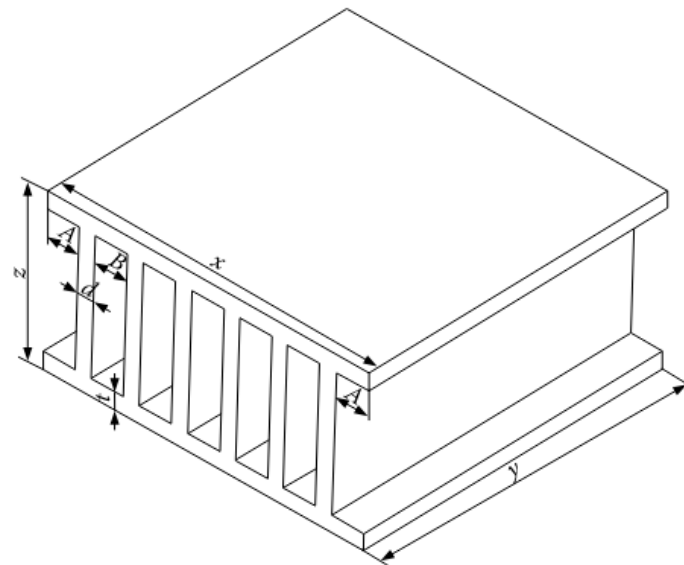


Figure 4. An additively manufactured one-piece solar panel. From [42], originally published under a CC-BY license.

Generally, diverse parts of microsattellites have been prepared by metal additive manufacturing, interestingly not only in the laboratory, but also by companies such as Rocket Lab, SpaceX, or Blue Origin [43–45]. For the future, even printing directly in space was announced [46], indicating that this area of additive manufacturing for microsattellites has already reached a certain process maturity.

While not much progress has been reported throughout the last year regarding metal additive manufacturing of microsattellites, many studies investigated the use of metal additive manufacturing for different parts of rockets, spaceships, etc. which will be discussed in the next sections.

4. Thrusters

Thrusters can be categorized based on diverse working principles, such as Hall thrusters showing a high thrust efficiency and high ion beam density due to a moderate

magnetic field applied to the acceleration zone [47], pulsed plasma thrusters [48], electro-spray thrusters working with ionic liquid propellants [49,50], etc. While Hall thrusters are most often used for satellites [51], applications requiring lower energies, such as the aforementioned CubeSats or other microsattellites, can be driven and navigated by microcathode arc or other plasma thrusters, field emission thrusters, electro-spray thrusters, or different sorts of electric thrusters [52–55].

One of the important differences between conventional production methods and additive manufacturing is the possibility to use more lightweight designs, but on the other hand to ensure the reliability of the 3D printed object in spite of possible differences in the mechanical or other physical properties, as compared to subtractive manufacturing methods. Meisel et al. and Woods et al., e.g., discussed the redesign of a NASA thruster applied for spacecraft attitude control, as it is enabled by switching from conventional manufacturing to powder-bed fusion of the metal alloy Inconel[®]718 [56,57]. They applied different specific designs for additive manufacturing and showed that manufacturing time and costs could be reduced by the new freedom of design, given by the additive manufacturing process. The same material was investigated by Soller et al. who also tested stainless steel 316 L and CoCr for high-temperature applications in a liquid rocket engine injector, especially an injector head for an expander cycle and a gas generator setup, finding a large potential mass reduction of approximately 25% due to an optimized design and significantly reduced manufacturing costs for the selective laser melting process [58].

Different designs were also discussed by Borgue et al. who compared a design for a gridded ion thruster with full design freedom with a second one taking into account limitations of additive manufacturing and found that only the latter could be manufactured [59]. Figure 5 depicts the design for the maximized thruster performance (Figure 5a) and the more realistic design, taking into account material and geometry limitations, e.g., disregarding multimaterial structures. While the latter is less innovative, it can be manufactured according to recent technological methods. However, new developments may enable additive manufacturing of the first design, too, which would lead to higher perceived performance because of the rounder chamber shape.

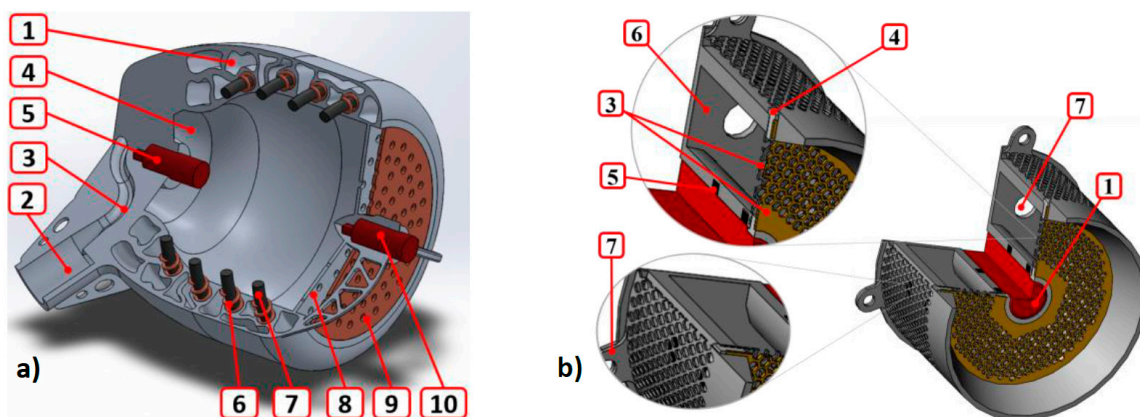


Figure 5. (a) Free design for maximized thruster performance; (b) design taking into account realistic additive manufacturing limitations. (1) Aluminum chamber, (2) connecting point importing the propellant, (3) channels guiding the gas, (4) gas exit, (5/10) hollow cathode for plasma generation, (6) electromagnet copper coil, (7) electromagnet iron core, (8/9) exit grids. From [59], originally published under a CC-BY-NC-ND license.

Besides the aforementioned materials, several metals and metal alloys were investigated as possible 3D printing materials for thrusters. Inconel[®]625 was chosen by Takahashi et al. who developed a thruster for the use with hydrazine based on binder jetting 3D printing to reduce the surface roughness as compared to laser-based additive manufacturing techniques [60]. In this way, production time and complexity could be reduced; vibration tests showed an equivalent performance of the 3D printed parts in compari-

son with flight-proven models, and hot-firing tests showed stable combustion, while the pressure roughness was slightly larger than in conventionally produced thrusters.

Another material class often used for aerospace applications is titanium aluminide alloys, containing the ordered γ -TiAl phase [61]. Seidel et al. used electron beam melting combined with laser metal deposition to produce a thruster nozzle from γ -TiAl for a cold-gas propulsion system, which can be used for navigation of small satellites to nanosatellites [62,63]. The authors pointed out the necessity to use a material that could withstand temperatures of more than 700 °C, which are necessary to increase the propellant efficiency in cold-gas propulsion systems [64]. Furthermore, either investigations of the interaction between γ -TiAl and the often used propellant ammonia are necessary [65], or noble gases should be used as propellants instead [66].

Tommila et al. investigated laser powder bed fusion of a nickel alloy for the production of very small nozzles with diameters below 1 mm, as they are used in electrothermal or chemical thrusters of small satellites [67]. They found typical printing-derived surface features of the as-printed nozzles to cause shock wave reflections and other thrust losses in comparison with conventionally produced nozzles of similar surface roughness, and suggest postprocessing of the nozzle exit cone to avoid such shock-inducing protrusions.

Powder bed laser processing was also used to prepare specimens from platinum rhodium alloy as well as tantalum and tungsten, finding that platinum rhodium additively manufactured parts could be used to build a combustion chamber and nozzle [68]. The authors suggest building the inner surface of a thrust chamber from noble metal alloys such as platinum rhodium or platinum iridium, while the outer wall could be prepared from tantalum and tungsten.

Sangregorio et al. used selective laser melting to produce grids and keeper electrodes in ion thrusters from molybdenum and found the surface roughness to be problematic, but manageable by postprocessing, and the mechanical properties to reach about 80% of those gained with conventional production techniques [69]. Similarly, Guo et al. described SLM used for the production of ion engine grids as well as for printing ion extraction systems and ion optics [70].

Miniaturized Hall thrusters were built by Olano et al. using SmCo permanent magnets to create the necessary magnetic field even under high temperatures and a 3D printed anode from stainless steel 316, produced by selective laser melting of a more complex design than possible with conventional techniques [71]. As Figure 6 shows, the anode design significantly influences the propellant distribution, so that more sophisticated 3D printing enables tailoring the propellant distribution more homogeneously than that of equipment prepared by traditional manufacturing.

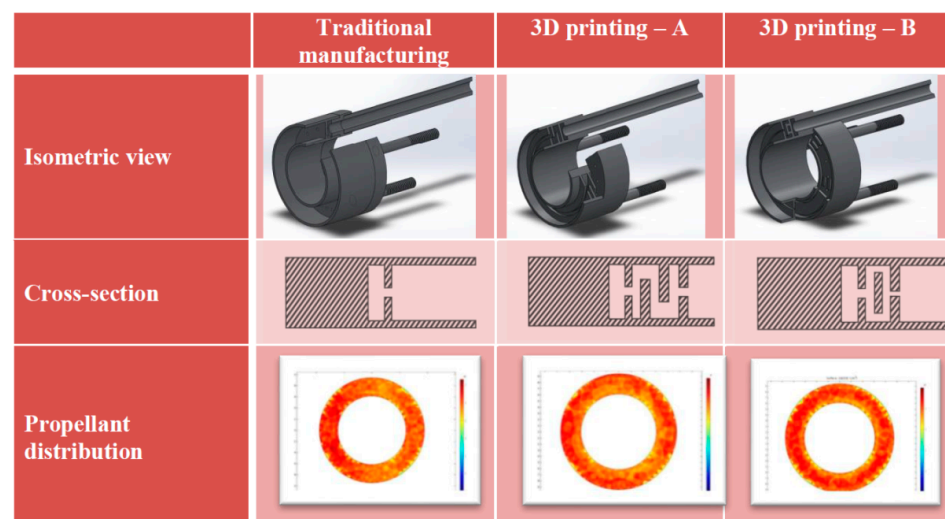


Figure 6. Anode designs with corresponding propellant distributions. From [71], originally published under a CC-BY license.

Another aspect, the reduction of manufacturing costs, was in the focus of a recent study of Hoffman and Grubisic who combined selective laser melting with off-the-shelf components to build a 20 cm-diameter microwave discharge ion thruster [72]. They found the ion production cost sufficient, while the mass utilization efficiency needed more future research to increase the thruster performance.

In these and many other studies, investigating possibilities to use metal additive manufacturing for the preparation of thruster parts [73–77] report that the main problems are related to the reduced mechanical properties in comparison with wrought material and the necessity to postprocess the printed parts to reduce undesired surface roughness or printing artifacts. However, as these examples show, there are already well-working processes and several materials that can be used for this purpose, so that further implementations especially in CubeSats and other microsatellites and smaller satellites can be expected in the near future.

Besides these technologies typically used in satellites, it is also possible to use different alloys for liquid rocket channel-wall nozzles [78,79] and other liquid rocket engine component applications [80,81], as well as to prepare composite propellant grains for solid rockets [82,83].

5. Structural Components

Structural parts of spacecraft have to show sufficient mechanical properties, combined with the necessity to withstand harsh conditions, especially regarding outer parts of satellites, rockets, etc. Metal 3D printing in general can be used to combine these necessities with the possibility to build lightweight structures and possibly even to use a modular design to enable change and service of single components [84]. Further, it can make fabrication quite fast, which was demonstrated by Orme et al. who used direct metal laser sintering to design, optimize, prepare, test, and finally launch different $AlSi_{10}Mg$ components for a satellite within half a year [85–87]. The process included mass optimization by a bionic design of the parts, optimized in several cycles.

Important parts of the construction of satellites are metal brackets connecting the satellite body with reflectors and feeder facilities. Allevi et al. performed a thermoelastic stress analysis on such brackets, produced by electron beam melting from a titanium-based alloy [88]. This analysis was applied to investigate the difference between CAD constructed and printed components. The method applied for this investigation, thermoelastic stress analysis, is based on thermal motions in a material due to dynamical load at a suitable frequency, made visible by a thermocamera. Results of the experimental investigation are depicted in Figure 7, showing the stress concentration in Figure 7a and opposite stress components on the upper and lower curvature in Figure 7b.

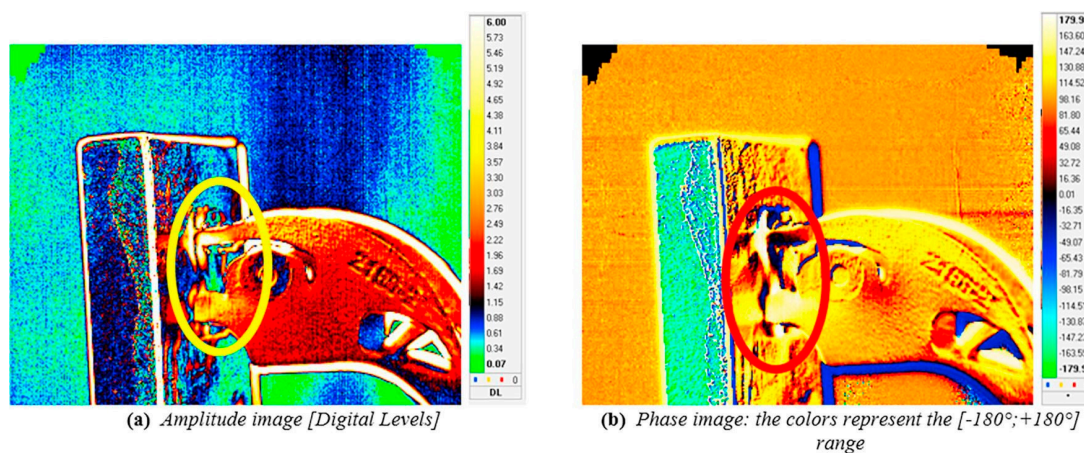


Figure 7. Thermoelastic stress analysis results revealing the location and the sign of the stress concentrations in a metal bracket for satellites. Reprinted from [88], with permission from Elsevier. (a) Amplitude image (digital levels); (b) phase image, the colors represent the range (-180° , $+180^\circ$).

Zhang et al. reported on vibration tests performed on $\text{AlSi}_{10}\text{Mg}$ manufactured by direct metal laser melting to form a lightweight satellite structure based on lattice sandwich panels, with a mass reduction of more than 50% as compared to conventionally produced satellite structures [89]. Similar mass reductions of around up to 50% can also be found for the previously applied laser beam melting technology in the space industry, often working with aluminum alloys. Begoc et al. compared laser beam melting of the often used $\text{AlSi}_7\text{Mg}_{0.6}$ with a new high-strength alloy named Scalmalloy[®] and developed the optimized parameters for the additive manufacturing process, resulting in better fatigue performance of Scalmalloy[®] in alternated traction compression up to 10^4 cycles and very low porosity rate, making it a promising material for the space industry [90].

It should be mentioned that while these results are often highly promising, space industry companies have to ensure that structural components will not be damaged under the extreme conditions in space, so that extended tests are performed before additively manufactured structural components are really sent into space, and only few of such components have been used in satellites, etc. [91–93]. This is different for elements with lower requirements according their mechanical properties, such as antennas.

6. Antennas

Telecommunication satellites need to enable high data transmission rates, resulting in the necessity to have large bandwidth and high power levels, which require special antenna designs with many horns per antenna. These complex design requirements suggest the use of additive manufacturing. Kilian et al. compared conventional and additive manufacturing of waveguides and radio frequency (RF) components, combining different components to reduce mass and power loss [94]. They found elliptical cross-sections to be advantageous for waveguides, with lower losses as compared to conventional rectangular waveguides. While linear polarization showed good antenna quality, the accuracy of circularly polarized waveguide components has to be further increased.

Gill et al. used direct metal laser sintering of $\text{AlSi}_{10}\text{Mg}$ to prepare antenna feed arrays for the Ka band based on high-efficiency horns, which are typically used as feed elements in high-throughput satellites using multibeam antennas [95]. The antenna feed array constructed according to typical limitations of 3D printing, such as reduced use of support that can easily be removed by machining, rounding off sharp corners, etc., is depicted in Figure 8, mounted on a plate for tests in an anechoic chamber. The authors successfully performed RF tests at 27–30 GHz and found a first natural frequency of 502 Hz, which is in the correct range for space payload systems. Furthermore, mechanical tests showed adequate results, making such antenna feed arrays suitable for communication satellites.

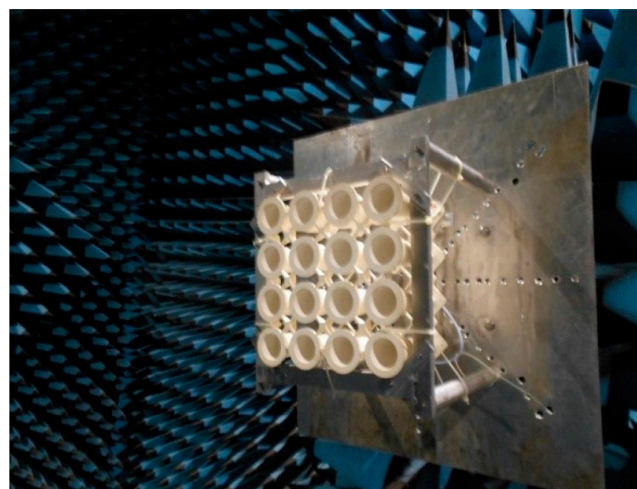


Figure 8. Direct metal laser sintered antenna feed array in an anechoic chamber. Reprinted from [95], with permission from Elsevier.

Instead of antennas, Peverini et al. investigated additively manufactured fifth- and sixth-order waveguide filters for the Ku/K band [96]. They compared filters prepared by selective laser melting of steel 1.2709 with silver plating, Ti₆Al₄V with silver plating, and the usual AlSi₁₀Mg with an SLA printed polymer with copper plating and found the latter be problematic due to the adhesion between metal plating and polymer base. All the prototypes, on the other side, showed sufficient RF reflection and transmission in the pass and stop bands, respectively, with the aluminum based waveguide filter showing the lowest insertion loss. Similarly, the group optimized dual-polarization waveguide components for the Ka-band, prepared by selective laser melting [97].

Other research groups concentrated on metamaterial filters for the K-band [98], waveguide antennas for the Ku band [99,100] or other bands [101,102]. Generally, here the mechanical and thermal requirements are less rigorous in comparison with the aforementioned applications; thus, most studies are based on state-of-the-art metal additive manufacturing, taking into account design for the respective technique and possibly a postprocessing step to avoid too high roughness. Because of these reduced requirements, additively manufactured antennas can be expected to be used in the near future.

7. Other Spacecraft Components

While the aforementioned components are recently most often prepared by metal additive manufacturing, there are some other possibilities to use these techniques for satellites or rockets and in future manned space missions.

Li et al., e.g., used selective laser melting of permalloy to prepare magnetic shields for fiber optic gyroscopes in spacecraft [103]. They found recrystallization annealing to improve the soft magnetic performance and the overall magnetic performance of the additively manufactured parts to be similar to traditional processing methods.

Taking a flow connector as an example, Borgue et al. suggested a design for additive manufacturing method especially for space applications [104]. While design for additive manufacturing usually takes into account the limitations of the 3D printing process, here also the functionality was discussed in different workshops and interviews with participating companies, resulting in a cost-efficient design and production method which is suggested to further reduce future development time and costs.

Other aspects taken into account are the general possibility to reduce space debris by proper additive manufacturing design of small satellites [105] or the idea of 3D printing in space, especially in the ISS or in future manned space missions to repair components [106]. Combining such promising attempts as the special design for additive manufacturing for space [104] with the potential advantages of reduced weight, time, and space debris can be expected to lead to an increase of 3D printing approaches for diverse spacecraft components.

8. Conclusions and Outlook

As this brief overview of recent developments in metal additive manufacturing shows, many satellite and spacecraft components can already be prepared by these 3D printing techniques, while several challenges still remain. Translating the fast progress of polymer- and metal-based additive manufacturing technologies and the steady development of new techniques into the near future, it can be assumed that many of the recent problems, e.g., related to surface roughness or insufficient mechanical properties, will be solved by the expected progress of the technologies themselves and by developing strategies to make new metals printable by these techniques.

An important point which has to be taken into account is the redesign for a specific additive manufacturing process, taking into account its limitations and making use of new freedom of design in order to optimize the mechanical, morphological, temperature-related, and other properties of the 3D printed objects.

Additionally, future research has to concentrate on further developing the 3D printing techniques described here in order to reduce shape deviations from the design and improve

the mechanical properties of additively manufactured objects toward the values reached by the wrought material. Further, optimizing the printing parameters for the materials especially well suited for space applications is necessary. In this way, it will be possible to reduce not only the mass of several components, but also development time and costs.

Author Contributions: Conceptualization, T.B., G.E. and A.E.; investigation, T.B., G.E. and A.E.; writing—original draft preparation, A.E.; writing—review and editing, T.B. and G.E. All authors have read and agreed to the published version of the manuscript.

Funding: This study was supported by the Silesian University of Technology Rector's Grant no. 14/030/RGJ21/00110.

Institutional Review Board Statement: Not applicable.

Informed Consent Statement: Not applicable.

Data Availability Statement: No data were created in this review.

Conflicts of Interest: The authors declare no conflict of interest. The funders had no role in the design of the study; in the collection, analyses, or interpretation of data; in the writing of the manuscript, or in the decision to publish the results.

References

1. Noorani, R. *Rapid Prototyping: Principles and Applications*; John Wiley & Sons: Hoboken, NJ, USA, 2005.
2. Murr, L.E.; Gaytan, S.M.; Ramirez, D.A.; Martinez, E.; Hernandez, J.; Amato, K.N.; Shindo, P.W.; Medina, F.R.; Wicker, R.B. Metal Fabrication by Additive Manufacturing Using Laser and Electron Beam Melting Technologies. *J. Mater. Sci. Technol.* **2012**, *28*, 1–14. [[CrossRef](#)]
3. Schmelzle, J.; Kline, E.V.; Dickman, C.J.; Reutzel, E.W.; Jones, G.; Simpson, T.W. (Re)Designing for Part Consolidation: Understanding the Challenges of Metal Additive Manufacturing. *J. Mech. Des.* **2015**, *137*, 111404. [[CrossRef](#)]
4. Plocher, J.; Panesar, A. Review on design and structural optimisation in additive manufacturing: Towards next-generation lightweight structures. *Mater. Des.* **2019**, *183*, 108164. [[CrossRef](#)]
5. Chen, Q.; Liu, J.K.; Liang, X.; To, A.C. A level-set based continuous scanning path optimization method for reducing residual stress and deformation in metal additive manufacturing. *Comput. Methods Appl. Mech. Eng.* **2020**, *360*, 112719. [[CrossRef](#)]
6. Carpenter, K.; Tabei, A. On residual stress development, prevention, and compensation in metal additive manufacturing. *Materials* **2020**, *13*, 255. [[CrossRef](#)]
7. Nickels, L. AM and aerospace: An ideal combination. *Met. Powder Rep.* **2015**, *70*, 300–303. [[CrossRef](#)]
8. Milewski, J.O. *Additive Manufacturing of Metals*; Springer Series in Materials Science 258; Springer: Berlin/Heidelberg, Germany, 2017.
9. ASTM Committee F42 on Additive Manufacturing Technologies, and ASTM Committee F42 on Additive Manufacturing Technologies. Subcommittee F42. 91 on Terminology. In *Standard Terminology for Additive Manufacturing Technologies*; F2792-12a; ASTM International: Pennsylvania, PA, USA, 2012.
10. Körner, C. Additive manufacturing of metallic components by selective electron beam melting—A review. *Int. Mater. Rev.* **2016**, *61*, 361–377. [[CrossRef](#)]
11. Sigl, M.; Lutzmann, S.; Zaeh, M.F. Transient physical effects in electron beam sintering. In Proceedings of the 2006 International Solid Freeform Fabrication Symposium, Austin, TX, USA, 14 September 2006; pp. 397–405.
12. Lodes, M.; Guschlbauer, R.; Körner, C. Process development for the manufacturing of 99.94% pure copper via selective electron beam melting. *Mater. Lett.* **2015**, *143*, 298–301. [[CrossRef](#)]
13. Schwerdtfeger, J.; Körner, C. Selective electron beam melting of Ti-48Al-2Nb-2Cr: Microstructure and aluminium loss. *Intermetallics* **2014**, *49*, 29–35. [[CrossRef](#)]
14. Milberg, J.; Sigl, M. Electron beam sintering of metal powder. *Prod. Eng.* **2008**, *2*, 117–122. [[CrossRef](#)]
15. Ramsperger, M.; Mújica Roncery, L.; Lopez-Galilea, I.; Singer, R.F.; Theisen, W.; Körner, C. Solution heat treatment of the single crystal nickel-base superalloy CMSX-4 fabricated by selective electron beam melting. *Adv. Eng. Mat.* **2015**, *17*, 1486–1493. [[CrossRef](#)]
16. Sochalski-Kolbus, L.M.; Payzant, E.A.; Cornwell, P.A.; Watkins, T.R.; Babu, S.S.; Dehoff, R.R.; Lorenz, M.; Ovchinnikova, O.; Duty, C. Comparison of residual stresses in Inconel 718 simple parts made by electron beam melting and direct laser metal sintering. *Met. Mater. Trans. A Phys. Metall. Mater. Sci.* **2015**, *46*, 1419–1432. [[CrossRef](#)]
17. Gasser, A.; Backes, G.; Kelbassa, I.; Weisheit, A.; Wissenbach, K. Laser additive manufacturing: Laser metal deposition (LMD) and selective laser melting (SLM) in turbo-engine applications. *Laser Tech. J.* **2010**, *7*, 57–63. [[CrossRef](#)]
18. Murr, L.E.; Martinez, E.; Amato, K.N.; Gaytan, S.M.; Hernandez, J.; Ramirez, D.A.; Shindo, P.W.; Medina, F.; Wicker, R.B. Fabrication of Metal and Alloy Components by Additive Manufacturing: Examples of 3D Materials Science. *J. Mater. Res. Technol.* **2012**, *1*, 42–54. [[CrossRef](#)]

19. Faubert, F.M.; Springer, G.S. Measurement of the thermal conductivity of argon, krypton and nitrogen in the range 800–2000 K. *J. Chem. Phys.* **1972**, *57*, 2333–2340. [[CrossRef](#)]
20. Spears, T.G.; Gold, S.A. In-process sensing in selective laser melting (SLM) additive manufacturing. *Integr. Mater. Manuf. Innov.* **2016**, *5*, 16–40. [[CrossRef](#)]
21. Sing, S.L.; Tey, C.F.; Tan, J.H.K.; Huang, S.; Yeong, W.Y. 3D printing of metals in rapid prototyping of biomaterials: Techniques in additive manufacturing. In *Rapid Prototyping of Biomaterials*, 2nd ed.; Woodhead Publishing Series in Biomaterials: Cambridge, UK, 2020; pp. 17–40.
22. Mazzucato, F.; Avram, O.; Valente, A.; Carpanzano, E. Recent Advances toward the Industrialization of Metal Additive Manufacturing. In *Systems Engineering in the Fourth Industrial Revolution*; John Wiley & Sons, Ltd.: Hoboken, NJ, USA, 2019; pp. 273–319. ISBN 978-1-119-51395-7.
23. Szost, B.A.; Terzi, S.; Martina, F.; Boisselier, D.; Prytuliak, A.; Pirling, T.; Hofmann, M.; Jarvis, D.J. A comparative study of additive manufacturing techniques: Residual stress and microstructural analysis of CLAD and WAAM printed Ti–6Al–4V components. *Mater. Des.* **2016**, *89*, 559–567. [[CrossRef](#)]
24. Barroqueiro, B.; Andrade-Campos, A.; Valente, R.A.F.; Neto, V. Metal Additive Manufacturing Cycle in Aerospace Industry: A Comprehensive Review. *J. Manuf. Mater. Process.* **2019**, *3*, 52. [[CrossRef](#)]
25. Resnina, N.; Palani, I.A.; Belyaev, S.; Mani Prabu, S.S.; Liulchak, P.; Karaseva, U.; Manikandan, M.; Jayachandran, S.; Bryukhanova, V.; Sahu, A.; et al. Structure, martensitic transformations and mechanical behavior of NiTi shape memory alloy produced by wire arc additive manufacturing. *J. Alloys Compd.* **2021**, *851*, 156851. [[CrossRef](#)]
26. Warsi, R.; Kazmi, K.H.; Chandra, M. Mechanical properties of wire and arc additive manufactured component deposited by a CNC controlled GMAW. *Mater. Today Proc.* **2021**, in press. [[CrossRef](#)]
27. Wen, Y.J.; Zhang, B.C.; Lakshmi Narayan, R.; Wang, P.; Song, X.; Zhao, H.; Ramamurty, U.; Qu, X.H. Laser powder bed fusion of compositionally graded CoCrMo-Inconel 718. *Addit. Manuf.* **2021**, *40*, 101926. [[CrossRef](#)]
28. Chandra, S.; Tan, X.P.; Lakshmi Narayan, R.; Descoins, M.; Mangelinck, D.; Beng Tor, S.; Liu, E.; Seet, G. Nanometer-scale precipitations in a selective electron beam melted nickel-based superalloy. *Scr. Mater.* **2021**, *194*, 113661. [[CrossRef](#)]
29. Allevi, G.; Capponi, L.; Castellini, P.; Chiariotti, P.; Cocchio, F.; Freni, F.; Marsili, R.; Martarelli, M.; Montanini, R.; Pasinetti, S.; et al. Investigating additive manufactured lattice structures: A multi-instrument approach. *IEEE Trans. Instrum. Meas.* **2020**, *69*, 2459–2467. [[CrossRef](#)]
30. Edwards, P.; O’Conner, A.; Ramulu, M. Electron beam additive manufacturing of titanium components: Properties and performance. *J. Manuf. Sci. Eng.* **2013**, *135*, 061016. [[CrossRef](#)]
31. Chandra, S.; Tan, X.P.; Lakshmi Narayan, R.; Wang, C.C.; Tor, S.B.; Seet, G. A generalized hot cracking criterion for nickel-based superalloys additively manufactured by electron beam melting. *Addit. Manuf.* **2021**, *37*, 101633.
32. Chen, Y.; He, Z.; Zhou, D.; Yu, Z.; Li, S. Integrated guidance and control for microsatellite real-time automated proximity operations. *Acta Astronaut.* **2018**, *148*, 175–185. [[CrossRef](#)]
33. Schulte, P.Z.; Spencer, D.A. Development of an integrated spacecraft guidance, navigation, & control subsystem for automated proximity operations. *Acta Astronaut.* **2016**, *118*, 168–186.
34. Blachowicz, T.; Pajak, K.; Recha, P.; Ehrmann, A. 3D printing for microsatellites—Material requirements and recent developments. *AIMS Mater. Sci.* **2020**, *7*, 926–938. [[CrossRef](#)]
35. Funase, R.; Ikari, S.; Miyoshi, K.; Kawabata, Y.; Nakajima, S.; Nomura, S.; Funabiki, N.; Ishikawa, A.; Kakihara, K.; Matsushita, S.; et al. Mission to Earth–Moon Lagrange Point by a 6U CubeSat: EQUULEUS. *IEEE Aerosp. Electron. Syst. Mag.* **2020**, *35*, 30–44. [[CrossRef](#)]
36. Synder, N.B. Design, Validation, and Verification of the Cal Poly Educational CubeSat Kit Structure. Master’s Thesis, California Polytechnic State University, San Luis Obispo, CA, USA, 2020. [[CrossRef](#)]
37. Yendler, B.; Meginnis, A.; Reif, A. Thermal management for high power Cubesats. In Proceedings of the 34th Annual AIAA/USU Small Satellite Conference 2020, ALL2020, Logan, UT, USA, 28 July 2020; p. 41. Available online: <https://digitalcommons.usu.edu/smallsat/2020/all2020/41/> (accessed on 10 November 2021).
38. Panagopoulos, J.A. Development of a CubeSat Power Management Subsystem for the ALSat#1 Mission. Ph.D. Thesis, Universidade da Beira Interior, Covilha, Portugal, 2020.
39. Alhammad, A.; Jarrar, F.; Marpu, P. Manufacturing, Analysis and testing of an additively manufactured nanosatellite structure. In Proceedings of the 2020 Advances in Science and Engineering Technology International Conferences (ASET), Dubai, United Arab Emirates, 4 February–9 April 2020; pp. 1–5.
40. Arnaud, E.; Dugenet, J.; Elis, K.; Girardot, A.; Guihard, D.; Menudier, C.; Monediere, T.; Roziere, F.; Thevenot, M. Compact isoflux X-band payload telemetry antenna with simultaneous dual circular polarization for LEO satellite applications. *IEEE Antennas Wirel. Propag. Lett.* **2020**, *19*, 1679–1683. [[CrossRef](#)]
41. Yurduseven, O.; Lee, C.; Gonzalez-Ovejero, D.; Ettorre, M.; Sauleau, R.; Chattopadhyay, G.; Fusco, V.; Chahat, N. Multi-beam Si/GaAs holographic metasurface antenna at W-band, *IEEE Trans. Antennas Propag.* **2021**, *69*, 3523–3528. [[CrossRef](#)]
42. Teng, L.; Zheng, X.D.; Jin, Z.H. Performance optimization and verification of a new type of solar panel for microsatellites. *Int. J. Aerosp. Eng.* **2019**, *2019*, 2846491. [[CrossRef](#)]

43. Winick, E. Rocket Lab: The Small Firm that Launched the 3D-Printed Space Revolution. 2019. Available online: <https://www.technologyreview.com/2019/06/19/134877/rocket-lab-the-small-firm-that-launched-the-3d-printed-space-revolution/> (accessed on 6 December 2021).
44. Thryft, A.R. SpaceX Reveals 3D-Printed Rocket Engine Parts. 2014. Available online: <https://www.designnews.com/design-hardware-software/spacex-reveals-3d-printed-rocket-engine-parts> (accessed on 6 December 2021).
45. Sher, D. Blue Origin 3D Printed BE-7 Engine Confirms Capability to LAND on Moon. 2020. Available online: <https://www.3dprintingmedia.network/blue-origin-3d-printed-be-7-engine-testing-confirms-capability-to-land-on-the-moon/> (accessed on 6 December 2021).
46. Walker, D. Rocket Lab Helping NASA 3D Print Spacecraft Parts in Orbit. 2019. Available online: <https://www.nzherald.co.nz/nz/rocket-lab-helping-nasa-3d-print-spacecraft-parts-in-orbit/JA4Q4IZW7IH5GAI TZVWYER2JZE/> (accessed on 6 December 2021).
47. Yamamoto, N.; Komurasaki, K.; Arakawa, Y. Discharge current oscillation in Hall thrusters. *J. Propuls. Power* **2005**, *21*, 870–876. [[CrossRef](#)]
48. Keidar, M.; Boyd, I.D.; Antonsen, E.L.; Gulczinski, F.S., III; Spanjers, G.G. Propellant charring in pulsed plasma thrusters. *J. Propuls. Power* **2004**, *20*, 978–984. [[CrossRef](#)]
49. Uchizono, N.M.; Collins, A.L.; Thuppul, A.; Wright, P.L.; Eckhardt, D.Q.; Ziemer, Z.; Wirz, R.E. Emission modes in electrospray thrusters operating with high conductivity ionic liquids. *Aerospace* **2020**, *7*, 141. [[CrossRef](#)]
50. Magnusson, J.M.; Collins, A.L.; Wirz, R.E. Polyatomic ion-induced electron emission (IIEE) in electrospray thrusters. *Aerospace* **2020**, *7*, 153. [[CrossRef](#)]
51. Boeuf, J.-P. Tutorial: Physics and modeling of Hall thrusters. *J. Appl. Phys.* **2017**, *121*, 011101. [[CrossRef](#)]
52. Mazouffre, S. Electric propulsion for satellites and spacecraft: Established technologies and novel approaches. *Plasma Sources Sci. Technol.* **2016**, *25*, 033002. [[CrossRef](#)]
53. Tummala, A.R.; Dutta, A. An overview of Cube-Satellite propulsion technologies and trends. *Aerospace* **2017**, *4*, 58. [[CrossRef](#)]
54. Levchenko, I.; Keidar, M.; Cantrell, J.; Wu, Y.-L.; Kuninaka, H.; Bazaka, K.; Xu, S. Explore space using swarms of tiny satellites. *Nat. Cell Biol.* **2018**, *562*, 185–187. [[CrossRef](#)] [[PubMed](#)]
55. Gallo, G.; Isoldi, A.; del Gatto, D.; Savino, R.; Capozzoli, A.; Curcio, C.; Liseno, A. Numerical aspects of particle-in-cell simulations for plasma-motion modeling of electric thrusters. *Aerospace* **2021**, *8*, 138. [[CrossRef](#)]
56. Meisel, N.A.; Woods, M.R.; Simpson, T.W.; Dickman, C.J. Redesigning a reaction control thruster for metal-based additive manufacturing: A case study in design for additive manufacturing. *J. Mech. Des.* **2017**, *139*, 100903. [[CrossRef](#)]
57. Woods, M.R.; Meise, N.A.; Simpson, T.W.; Dickman, C.J. Redesigning a reaction control thruster for metal-based additive manufacturing: A case study in design for additive manufacturing. In Proceedings of the ASME 2016 International Design Engineering Technical Conferences and Computers and Information in Engineering Conference, Volume 2A: 42nd Design Automation Conference, Charlotte, NC, USA, 21–24 August 2016. [[CrossRef](#)]
58. Soller, S.; Beyer, S.; Dahlhaus, A.; Konrad, A.; Kretschmer, J.; Rackemann, N.; Zeiss, W. Development of liquid rocket engine injectors using additive manufacturing. In Proceedings of the 6th European Conference for Aerospace Sciences (EUCASS 2015), Krakow, Poland, 30 July 2015; p. 31.
59. Borgue, O.; Valjak, F.; Panarotto, M.; Isaksson, O. Supporting additive manufacturing technology development through constraint modelling in early conceptual design: A satellite propulsion case study. In Proceedings of the Design Society: DESIGN Conference, Cavtat, Croatia, 1 May 2020; pp. 817–826. [[CrossRef](#)]
60. Takahashi, M.; Morita, N.; Matsuura, Y. Development status of 4N class low-cost thrusters made of 3D-printed metals. In Proceedings of the Joint Symposium 32nd ISTS & 9th NSAT 2019, Tomioka, Japan, 15–21 June 2019; Available online: <https://www.meeting-schedule.com/ists2019/pdf/2019-a-04.pdf> (accessed on 10 November 2021).
61. Bewlay, B.P.; Weimer, M.; Kelly, T.; Suzuki, A.; Subramanian, P.R. The science, technology, and implementation of TiAl alloys in commercial aircraft engines. *MRS Online Proc.* **2013**, *1516*, 49–58. [[CrossRef](#)]
62. Seidel, A.; Saha, S.; Maiwald, T.; Moritz, J.; Polenz, S.; Marquardt, A.; Kaspar, J.; Finaske, T.; Lopez, E.; Brueckner, F.; et al. Intrinsic heat treatment within additive manufacturing of gamma titanium aluminide space hardware. *JOM* **2019**, *71*, 1513–1519. [[CrossRef](#)]
63. Seidel, A.; Lopez, E.; Saha, S.; Maiwald, T.; Moritz, J.; Polenz, S.; Marquardt, A.; Kaspar, J.; Finaske, T.; Riede, M.; et al. Hybrid additive manufacturing of gamma titanium aluminide space hardware. In Proceedings of the Material Science and Technology (MS&T) 2018, Columbus, OH, USA, 14–18 October 2018.
64. Gilpin, M.; Scharfe, D.; Young, M.; Pancotti, A. Molten Boron Phase-Change Thermal Energy Storage to Augment Solar Thermal Propulsion Systems. In Proceedings of the 47th AIAA/ASME/SAE/ASEE Joint Propulsion Conference & Exhibit (American Institute of Aeronautics and Astronautics), San Diego, CA, USA, 31 July–3 August 2011. [[CrossRef](#)]
65. Zhao, B.; Sun, J.; Wu, J.S.; Yuan, Z.X. Gas nitriding behavior of TiAl based alloys in an ammonia atmosphere. *Scr. Mater.* **2002**, *46*, 581–586. [[CrossRef](#)]
66. Kelley, R.L.; Jarkey, D. CubeSat Material Limits for Design for Demise. In *AIAA SPACE 2015 Conference and Exposition*; Springer: Berlin/Heidelberg, Germany, 2015. [[CrossRef](#)]
67. Tommila, C.D.; Hartsfield, C.R.; Redmond, J.J.; Komives, J.R. Performance Impacts of Metal Additive Manufacturing of Very Small Nozzles. *J. Aerosp. Eng.* **2021**, *34*, 04020115. [[CrossRef](#)]

68. Wermuth, L.; Beyer, S.; Sebald, T.; Deck, J.; Kraus, S.; Reiß, F.; Brückner, F.; Seidel, A.; Humm, S.; Pambaguian, L.; et al. Selective laser melting of noble and refractory alloys for next generation spacecraft thruster. In Proceedings of the Metallic Materials and Processes: Industrial Challenges—MMP 2015, Deauville, France, 25–27 November 2015.
69. Sangregorio, M.; Xie, K.; Wang, N.F.; Zhang, Z.; Qin, Y. 3D Printed molybdenum for grids and keeper electrodes in ion thruster. In Proceedings of the 15th Spacecraft Charging Technology Conference, Kobe, Japan, 25–29 June 2018.
70. Guo, N.; Xie, K.; Sangregorio, M.; Wang, N.F.; Zhang, Z.; Gabriel, S.B. 3D printing of ion optics for electric propulsion. *Front. Phys.* **2019**, *6*, 145. [[CrossRef](#)]
71. Olano, A.; Ren, J.; Zhang, G.; Tang, H.; Zhang, T.; Li, J. Improvements in miniaturized Hall Thrusters by use of high-temperature SmCo magnets and additive manufacturing techniques. *IOP Conf. Ser. Mater. Sci. Eng.* **2019**, *576*, 012002. [[CrossRef](#)]
72. Hoffman, D.; Grubisic, A. Discharge-mode testing of the X-EPT microwave ECR gridded ion thruster. In Proceedings of the 36th International Electric Propulsion Conference, Vienna, Austria, 15–20 September 2019.
73. Essa, K.; Hassanin, H.; Attallah, M.M.; Adkins, N.J.; Musker, A.J.; Roberts, G.T.; Tenev, N.; Smith, M. Development and testing of an additively manufactured monolithic catalyst bed for HTP thruster applications. *Appl. Catal. A Gen.* **2017**, *542*, 125–135. [[CrossRef](#)]
74. Romei, F.; Grubisic, A.N. Validation of an additively manufactured resistojet through experimental and computational analysis. *Acta Astronaut.* **2020**, *167*, 14–22. [[CrossRef](#)]
75. Ngwu, G.O.; Ugheoke, B.I.; Yusuf, O.T.; Nyabam, M.A.; Onuh, S.O. Numerical analysis and modelling of a 100 N hypergolic liquid bipropellant thruster. *Adv. Aerosp. Sci. Technol.* **2020**, *5*, 85–99. [[CrossRef](#)]
76. Hopping, E.P.; Huang, W.S.; Xu, K.G. Small Hall effect thruster with 3D printed discharge Channel: Design and thrust measurements. *Aerospace* **2021**, *8*, 227. [[CrossRef](#)]
77. Kerstens, F.; Cervone, A.; Gradl, P. End to end process evaluation for additively manufactured liquid rocket engine thrust chambers. *Acta Astronaut.* **2021**, *182*, 454–465. [[CrossRef](#)]
78. Gradl, P.R.; Protz, C.; Wammen, T. Additive manufacturing and hot-fire testing of liquid rocket channel wall nozzles using blown powder directed energy deposition Inconel 625 and JBK-75 alloys. AIAA 2019-4362. In Proceedings of the AIAA Propulsion and Energy 2019 Forum, Indianapolis, IN, USA, 19–22 August 2019.
79. Gradl, P.R. Rapid fabrication techniques for liquid rocket channel wall nozzles. AIAA 2016-4771. In Proceedings of the 52nd AIAA/SAE/ASEE Joint Propulsion Conference, Salt Lake City, UT, USA, 25–27 July 2016.
80. Katsarelis, C.; Chen, P.; Gradl, P.; Protz, C.; Jones, Z.; Ellis, D.; Evans, L. Additive manufacturing of NASA HR-1 material for liquid rocket engine component applications. In Proceedings of the Joint Army-Navy-NASA-Air Force (JANNAF), Tampa, FL, USA, 9–13 December 2019; Available online: <https://ntrs.nasa.gov/archive/nasa/casi.ntrs.nasa.gov/20200001007.pdf> (accessed on 10 November 2021).
81. Patel, N.; Standbridge, S.; van den Berghe, M.; Devalaraju, V. Design and additive manufacturing considerations for liquid rocket engine development. AIAA 2019-4392. In Proceedings of the AIAA Propulsion and Energy 2019 Forum, Indianapolis, IN, USA, 19–22 August 2019.
82. Chandru, R.A.; Balasubramanian, N.; Oommen, C.; Raghunandan, B.N. Additive manufacturing of solid rocket propellant grains. *J. Propuls. Power* **2018**, *34*, 1090–1093. [[CrossRef](#)]
83. Ozawa, K.; Wang, H.-w.; Yoshino, T.; Tsuboi, N. Time-resolved fuel regression measurement function of a hybrid rocket solid fuel integrated by multi-material additive manufacturing. *Acta Astronaut.* **2021**, *187*, 89–100. [[CrossRef](#)]
84. Borgue, O.; Panarotto, M.; Isaksson, O. Modular product design for additive manufacturing of satellite components: Maximising product value using genetic algorithms. *Concurr. Eng.* **2019**, *27*, 331–346. [[CrossRef](#)]
85. Orme, M.E.; Gschweidl, M.; Vernon, R.; Ferrari, M.; Madera, I.J.; Yancey, R.; Mouriaux, F. A demonstration of additive manufacturing as an enabling technology for rapid satellite design and fabrication. In Proceedings of the International SAMPE Technical Conference, Long Beach, CA, USA, 23–26 May 2016; pp. 23–26.
86. Orme, M.E.; Gschweidl, M.; Ferrari, M.; Vernon, R.; Madera, I.J.; Yancey, R.; Mouriaux, F. Additive manufacturing of lightweight, optimized, metallic components suitable for space flight. *J. Spacecr. Rocket.* **2017**, *54*, 1050–1059. [[CrossRef](#)]
87. Orme, M.; Madera, I.; Gschweidl, M.; Ferrari, M. Topology optimization for additive manufacturing as an enabler for light weight flight hardware. *Design* **2018**, *2*, 51. [[CrossRef](#)]
88. Allevi, G.; Cibeca, M.; Fioretti, R.; Marsili, R.; Montanini, R.; Rossi, G. Qualification of additively manufactured aerospace brackets: A comparison between thermoelastic stress analysis and theoretical results. *Measurement* **2018**, *126*, 252–258. [[CrossRef](#)]
89. Zhang, X.Y.; Zhou, H.; Shi, W.H.; Zeng, F.M.; Zeng, H.Z. Vibration tests of 3D printed satellite structure made of lattice sandwich panels. *AIAA J.* **2018**, *56*, 4213–4217. [[CrossRef](#)]
90. Begoc, S.; Montredon, F.; Pommatau, G.; Leger, G.; Gas, M.; Eyriagnoux, S. Additive manufacturing of Scalmalloy® satellite parts. In Proceedings of the 8th European Conference for Aeronautics and Space Sciences (EUCASS), Madrid, Spain, 1–4 July 2019. [[CrossRef](#)]
91. RUAG Space: First 3D Printed Part Is Going to the Moon, RUAG. Available online: <https://www.ruag.com/en/news/ruag-space-first-3d-printed-part-going-moon> (accessed on 12 September 2021).
92. Airbus Defence and Space Optimising Components Using 3D Printing for New Eurostar E3000 Satellite Platforms, Airbus. Available online: <https://www.airbus.com/newsroom/press-releases/en/2015/03/airbus-defence-and-space-optimising-components-using-3d-printing-for-new-eurostar-e3000-satellite-platforms.html> (accessed on 12 September 2021).

93. Wall, M. Israel's Beresheet Spacecraft Crashes into Moon during Landing Attempt. Space.com. Available online: <https://www.space.com/israeli-beresheet-moon-landing-attempt-fails.html> (accessed on 12 September 2021).
94. Kilian, M.; Hartwanger, C.; Schneider, M.; Hatzenbichler, M. Waveguide components for space applications manufactured by additive manufacturing technology. *IET Microw. Antennas Propag.* **2017**, *11*, 1949–1954. [[CrossRef](#)]
95. Gill, S.S.; Arora, H.; Jidesh; Sheth, V. On the development of Antenna feed array for space applications by additive manufacturing technique. *Addit. Manuf.* **2017**, *17*, 39–46. [[CrossRef](#)]
96. Peverini, O.A.; Addamo, G.; Lumia, M.; Virone, G.; Calignano, F.; Lorusso, M.; Manfredi, D. Additive manufacturing of Ku/K-band waveguide filters: A comparative analysis among selective-laser melting and stereo-lithography. *IET Microw. Antennas Propag.* **2017**, *11*, 1936–1942. [[CrossRef](#)]
97. Addamo, G.; Peverini, O.A.; Manfredi, D.; Calignano, F.; Paonessa, F.; Virone, G.; Tascone, R.; Dassano, G. Additive manufacturing of Ka-band dual-polarization waveguide components. *IEEE Trans. Microw. Theory Tech.* **2018**, *66*, 3589–3596. [[CrossRef](#)]
98. Arsanjani, A.; Robins, L.; Teschl, R.; Bösch, W. Implementation of K-band Mushroom meta-material filter for satellite applications. In Proceedings of the 2020 50th European Microwave Conference (EuMC), Utrecht, The Netherlands, 12–14 January 2021; pp. 495–498.
99. García-Marín, E.; Masa-Campos, J.L.; Sánchez-Olivares, P.; Ruiz-Cruz, J.A. Evaluation of additive manufacturing techniques applied to Ku-band multilayer corporate waveguide antennas. *IEEE Antennas Wirel. Propag. Lett.* **2018**, *17*, 2114–2118. [[CrossRef](#)]
100. Sommer, A.; Schinagl-Weiß, A.; Hartwanger, C.; Kilian, M.; Schneider, M. Multiple spot beam reflector antenna for high throughput satellites using additive manufacturing technology. In Proceedings of the 2019 13th European Conference on Antennas and Propagation (EuCAP), Krakow, Poland, 31 March–5 April 2019; pp. 1–5.
101. Verploegh, S.; Coffey, M.; Grossman, E.; Popovic, Z. Properties of 50–110-GHz waveguide components fabricated by metal additive manufacturing. *IEEE Trans. Microw. Theory Tech.* **2017**, *65*, 5144–5153. [[CrossRef](#)]
102. Pohl, P.; Kilian, M.; Schinagl-Weiß, A.; Hartwanger, C. Additive manufacturing developments for satellite antenna applications from C- to Ka-band. In Proceedings of the 2019 12th German Microwave Conference (GeMiC), Stuttgart, Germany, 25–27 March 2019; pp. 222–225.
103. Li, B.; Zhang, L.; Fu, W.Q.; Xu, H.S. General investigations on manufacturing quality of permalloy via selective laser melting for 3D printing of customized magnetic shields. *JOM* **2020**, *72*, 2834–2844. [[CrossRef](#)]
104. Borgue, O.; Müller, J.; Leicht, A.; Panarotto, M.; Isaksson, O. Constraint replacement-based design for additive manufacturing of satellite components: Ensuring design manufacturability through tailored test artifacts. *Aerospace* **2019**, *6*, 124. [[CrossRef](#)]
105. Becedas, J.; Caparrós, A. Additive manufacturing applied to the design of small satellite structure for space debris reduction. In *Applications of Design for Manufacturing and Assembly*; Pacurar, A.C., Ed.; IntechOpen: London, UK, 2018; pp. 59–76.
106. Sears, P.J.; Ho, K. Impact evaluation of in-space additive manufacturing and recycling technologies for on-orbit servicing. *J. Spacecr. Rocket.* **2018**, *55*, 1498–1508. [[CrossRef](#)]